Hindawi
Advances in Polymer Technology
Volume 2019, Article ID 6090965, 13 pages
https://doi.org/10.1155/2019/6090965

Research Article

Development and *In-Vitro* Evaluation of pH Responsive Polymeric Nano Hydrogel Carrier System for Gastro-Protective Delivery of Naproxen Sodium

Rai Muhammad Sarfraz,[1] **Muhammad Rouf Akram**,[1] **Muhammad Rizwan Ali**,[1] **Asif Mahmood**,[2] **Muhammad Usman Khan**,[1] **Husnain Ahmad**,[1] **and Muhammad Naeem Qaisar**[1]

[1]*College of Pharmacy, University of Sargodha, Sargodha 40100, Punjab, Pakistan*
[2]*Department of Pharmaceutics, Faculty of Pharmacy, University of Lahore, Lahore, Pakistan*

Correspondence should be addressed to Rai Muhammad Sarfraz; sarfrazrai85@yahoo.com

Received 17 September 2019; Revised 8 November 2019; Accepted 21 November 2019; Published 29 December 2019

Guest Editor: Mingqiang Li

Current research work was carried out for gastro-protective delivery of naproxen sodium. Polyethylene glycol-g-poly (methacrylic acid) nanogels was developed through free radical polymerization technique. Formulation was characterized for swelling behaviour, entrapment efficiency, Fourier transform infrared (FTIR) spectroscopy, Differential scanning calorimetry (DSC), and Thermal Gravimetric Analysis (TGA), Powder X-ray diffraction (PXRD), Zeta size distribution, and Zeta potential measurements, and *in-vitro* drug release. pH dependent swelling was observed with maximum drug release at higher pH. PXRD studies confirmed the conversion of loaded drug from crystalline to amorphous form while Zeta size measurement showed size reduction. On the basis of these results it was concluded that prepared nanogels proved an effective tool for gastro-protective delivery of naproxen sodium.

1. Introduction

Naproxen, a propionic acid derivative, is widely used either in the form of free acid or sodium salt in the treatment of musculoskeletal and joint disorders. It is also used in management of headache including migraine, dysmenorrhoea, soft-tissue disorders, postoperative pain, and acute gout as well as antipyretic agent [1]. Along with the benefits, there are many gastro intestinal risk factors associated with chronic use of these agents, such as mucosal damage and development of peptic ulcers [2]. The inhibition of biosynthesis of endogenous prostaglandin by nonsteroidal anti-inflammatory drugs (NSAIDs) is the primary mechanism that leads to damage of the gastric mucosa [3]. Secondary to this mechanism, acid-mediated direct topical effect of NSAIDs also resulted into breakdown of mucosal defence by depletion of the mucus barrier [4–6]. Different strategies have been reported to modify the local damage of the gastric mucosa caused by NSAIDs thus reducing the complications. These include; prodrug formulation, complex formation with biocompatible materials, and varying the route of drug delivery thus decreasing local contact of these agents to the gastric mucosa [7–10]. Targeted delivery of NSAIDs to the intestine in the form of delayed release formulations provided the change in absorption site for these agents from stomach to intestine with reduced frequency of gastric ulceration [11]. Furthermore, decreasing the particle size and changing the drug from crystalline to amorphous form is also effective in order to minimize NSAIDs related complications to the gastric mucosa [5, 12].

Previously various techniques have been studied for gastro-protective delivery of NSAIDs [13]. In many studies application of nanogels carrier systems has been reported as tool for controlled and targeted delivery of pH sensitive therapeutic agents i.e. peptides and proteins through oral route in order to bypass gastric environment [14]. Due to this characteristic, nanogels carrier system is getting the attention of researchers for targeted delivery of NSAIDs. Nanogels are nano-scale

hydrogels particulate systems (hydrogel nanoparticles) that possess the characteristics of hydrogels as well as of nanoparticles at the same time [15, 16]. Furthermore, these systems are also a preferred tool for reducing the particle size of the drug [17, 18]. This novel drug delivery approach provided the enhancement in bioavailability of drugs as well as reduction in drug related side effects [14, 19, 20]. Moreover, Chemical cross-linking in nanogels enable these systems to retain their mechanical stability thus stably holding the loaded drug [21]. Many researchers have formulated nanogels drug carrier systems that are sensitive to external stimuli especially pH and temperature by employing several natural and synthetic biodegradable polymers. By modifying the properties of polymeric networks through conjugation with pH sensitive moiety, these systems have been enabled to release the active pharmaceutical moiety at specific pH in order to achieve targeted drug delivery [14].

Poly ethylene glycol (PEG) is a nontoxic, water soluble polymer that exhibits the resistance to recognition by the immune system and presented rapid clearance from the body. Due to these advantages, PEG based nanogels are considered good candidates as biomaterials for drug delivery. These systems have been used in drug delivery, wound healing, and a variety of other biomedical applications. These drug delivery systems are often used in combination with other polymers in order to prepare an appropriate biomaterial. Previously these systems have been studied extensively for targeted delivery of peptides and protein through oral route. PEG based systems also have been used as controlled release devices. The rate of drug release from these systems was found to be dependent not only on the method of preparation, but also on the crosslinking density, molecular weight of the PEG anionic chains, and drug solubility [22].

In the present work, PEG-6000 based pH sensitive nanogels are synthesized by grafting with methacrylic acid. These pH sensitive nanogels are then employed as a carrier system for targeted delivery of naproxen sodium in order to bypass gastric release of the drug. Such formulations will be helpful to provide gastro-protective effect through site specific drug delivery with reduced complications associated with chronic use of NSAIDs.

2. Materials and Methods

2.1. Chemicals. Naproxen sodium was obtained as a gift from the Global Pharmaceuticals Islamabad, Pakistan, PEG-6000 was gifted from the Trison Research Laboratories (Pvt.) Ltd., Sargodha, Pakistan, methacrylic acid and methylene bisacrylamide was purchased from Merck KGaA, Darmstadt, Germany. All other chemicals used were of analytical grade.

2.2. Preparation of Nanogels Particulate System of PEG and MAA. The polymer was mixed with monomer in different molar ratio. Methylene bisacrylamide was added as a cross linking agent in a suitable amount. This mixture was added to a three necked reaction flask supplied with inlet of nitrogen and continuous stirring on a hot plate magnetic stirrer at temperature 37°C. Nitrogen was purged continuously through this mixture for 30 minutes in order to remove the dissolved oxygen. Potassium persulfate (KPS) was then added to the mixture with continuous stirring in order to start polymerization. Formed mixture was poured to a test tube, sealed with aluminium foil and allowed to stand in a water bath at 70°C for 6 hrs. After completion of polymerization reaction, the prepared hydrogel was removed from the test tubes, cut into small slices, and washed with water–methanol mixture 50:50 thrice. Small slices of hydrogel were crushed in wet form and passed through suitable sieve in order to achieve particulate system of uniform size. Particulate systems were dried at 50°C in a hot air oven until constant weight and stored for further analysis [23–25]. Chemical structure of individual ingredients and formulations are presented in Figure 1. In a similar way with varying concentration of polymer, monomer, and cross linking agent, 9 formulations were prepared as presented in Table 1.

2.3. Drug Loading. The drug solution was prepared in 0.1 M phosphate buffer of pH 6.8 (USP). A known quantity of dried nanogels particulate were accurately weighed and immersed in the drug solution and placed at 25°C. After 48 hrs, pH of the solution was decreased to 1.2 by the addition of 0.1 M HCL solution for the locking of the drug loaded nanogels. The mixture was filtered and the residue was also washed with 100 mL of distilled water to remove unentrapped drug. Drug loaded nanogels were dried at low temperature in a hot air oven and stored for further analysis [26–28].

3. *In-Vitro* Characterization of Nanogels Particulate Systems

3.1. Product Yield. Product yield for different formulations was determined in order to evaluate the efficiency of the process with the help of Equations (1) and (2) [17],

$$\text{Product yield} = 100 - \text{Mass loss}, \tag{1}$$

$$\text{Mass loss (\%)} = \frac{M_o - M_1}{M_o} \times 100, \tag{2}$$

where, M_o = initial weight of all ingredients, M_1 = final weight of nanogels.

3.2. Calculation of Entrapment Efficiency. A known quantity of drug loaded nanogels were pulverized and added to 10 mL of 6.8 pH buffer solution and was subjected to stirring for 24 hrs at room temperature. The resulting suspension was filtered and the residue was washed with the same buffer solution. The filtrate drug contents were measured with the help of a double beam UV/Vis spectrophotometer at 332 nm. The entrapment efficiency and the percentage drug loading was calculated with the help of Equations (3) and (4) [29],

$$\text{Drug loading(\%)} = \frac{\text{Amount of drug in particles}}{\text{Amount of drug loaded particles}} \times 100, \tag{3}$$

$$\text{Entrapment efficiency(\%)} = \frac{\text{Actual loading}}{\text{Theoretical loading}} \times 100. \tag{4}$$

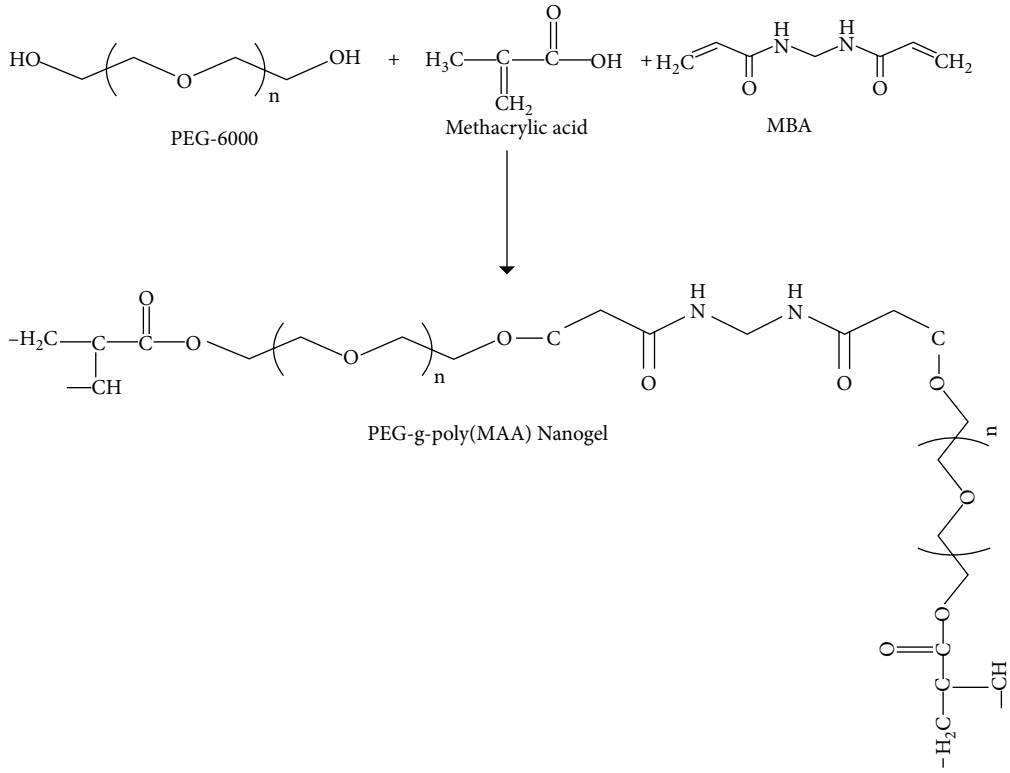

Figure 1: Proposed structure of PEG-g-poly (methacrylic acid) nanogels.

Table 1: Composition of PEG-g-poly (MAA) nanogels and calculation of sol–gel fraction.

Code	Ethylene glycol: MAA (mol)	Cross linker (% of total wt. of PEG + MAA)	Initiator (% of total wt. of PEG + MAA)	W_i (mg)	W_e (mg)	Sol fraction (%) $= \frac{W_i - W_e}{W_i} \times 100$	Gel fraction (%) = 100 − Sol fraction
N1	1:1	1	1	200	176	12	88
N2	2:1	1	1	200	162	19	81
N3	3 : 1	1	1	200	148	26	74
N4	1:2	1	1	200	181	9.5	90.5
N5	1:3	1	1	200	187	6.5	93.5
N6	1:4	1	1	200	191	4.4	95.5
N7	1:1	2	1	200	179	10.5	89.5
N8	1:1	3	1	200	186	7	93
N9	1:1	4	1	200	190.2	4.9	95.1

3.3. Sol–Gel Fraction Determination. The gel fraction of prepared formulations was determined with the help of the Soxhlet apparatus at 85°C for 12 hrs. Discs of hydrogel were cut into uniform small size slices, dried in a hot air oven at 50°C until constant weight and then subjected to extraction in distilled water. After the specified time, slices of hydrogel were taken off from the water and subjected to drying for 72 hrs at 50°C. By using the Equations (5) and (6), Sol fraction and gel fraction was calculated [30],

$$\text{Sol fraction} = \frac{M_i - M_e}{M_i} \times 100, \tag{5}$$

where M_i = initial mass, M_e = mass after extraction,

$$\text{Gel fraction} = 100 - \text{Sol fraction}. \tag{6}$$

3.4. Swelling Behaviour. Swelling index of the prepared formulations was studied in 0.1M buffer solutions of pH 1.2 and 6.8 while maintaining the temperature at 37°C. Weighed quantity of grafted nanogels particulate were taken in a tea bag and immersed in specified buffer solution. After a specific time interval the tea bags were removed from solution and excess of water was removed with the help of tissue paper and weighed on a weighing balance. This process was continued until constant weight. Degree of swelling (Q) of prepared formulations was calculated at different pH values by using Equation (7) [31],

$$Q = \frac{M_s}{M_d}, \tag{7}$$

where M_s = mass of swelled particles, M_d = mass of dried particles before immersing.

3.5. Micromeritic Properties. Micromeritic properties of prepared nanogels particulate system were determined in order to estimate the flow characteristics of formulations. Angle of repose, Bulk density, Tapped density, Carr's compressibility index, and Hausner's ratio was calculated as previously describe in study performed by Sarfraz et al. [25].

3.6. Particle Size Analysis. Average particle size of prepared nanogels particulate systems was evaluated with the help of particles size analyzer. For this purpose nanogels particulate systems were suspended in ultrapure water and particle size analysis was performed by the Particle size analyzer (Zetasizer Ver System; Malvern Instruments, Malvern, UK) using Dynamic Light Scattering (DLS) method [32, 33].

3.7. Zeta Potential Measurement. Measurement of Zeta potential of the drug loaded nanogels was also carried out in order to confirm the stability. Meanwhile, ionization of prepared formulation were also studied with the help of zeta potential.

3.8. FTIR Spectroscopy. FTIR spectra of PEG-6000, MAA, MBA, pure drug NPS, and drug loaded nanogels were measured between 400 and 4000 cm^{-1} with the help of IR spectrophotometer for the confirmation of grafting. For this purpose, samples were prepared by mixing the finely grounded prepared formulations with KBr and was placed on disc slit and the IR spectra was recorded [34].

3.9. Thermal Analysis. For the determination of thermal stability of ingredients in grafted nanogels, thermal analysis of individual ingredients and prepared formulations were performed through DSC and TGA. DSC of samples was performed under nitrogen environment by gradually applying heat stress from ambient to 400°C at the rate of 10°C/min while TGA analysis was performed in a temperature range of 0–800°C [25].

3.10. Powder X-Ray Diffraction Studies. Powder X-Ray diffraction studies of pure drug, polymers, and drug loaded formulations were performed and results were compared. Powder XRDs were calculated at 5–50°C at 2Θ in order to evaluate the crystalline or amorphous nature of the drug [35, 36].

3.11. In-Vitro Drug Release. A calibrated USP type-2 dissolution apparatus (Paddle apparatus) was used in order to perform the dissolution studies of drug loaded formulations at pH 1.2 and 6.8 respectively. 900 mL of each solution was used as a medium while maintaining the temperature at 37°C ± 0.2 and paddles speed at 50 rpm. At specified time intervals 5 mL of the samples were withdrawn and replaced with the same amount of fresh medium. The cumulative drug released was calculated by measuring the absorbance with the help of UV/Vis spectrophotometer at 332 nm. For each formulation, the same procedure was adopted to study the dissolution parameters [29].

3.12. Release Kinetics. By applying different model-dependent approaches, i.e. zero order, first order, Korsmeyer–Peppas and Higuchi, dissolution data from all prepared formulations were analyzed in order to study the kinetics of the drug release.

3.12.1. Zero-Order Model

$$M_t = K_o t. \tag{8}$$

In this equation, k_o represent the Zero-order rate constant while M_t is the amount of drug released at time t.

3.12.2. Higuchi Model. Where drug release is a function of square root of time, these systems are described under Higuchi model i.e. insoluble matrix,

$$M_t = K_H t^{1/2}, \tag{9}$$

where K_H represents the Higuchi rate constant.

3.12.3. Korsmeyer–Peppas Model. In order to evaluate the mode of drug release, the data of drug release were fitted to Korsmeyer–Peppas model as given,

$$\frac{M_t}{M_\infty} = K t^n, \tag{10}$$

where M_t/M_∞ = Fraction of drug released at time interval t, K = Rate constant of drug release, n = Drug release exponent.

The value of "n" calculated from this equation was used to describe the mode of drug release, as these are interrelated. If the value of "n" is greater than 0.89 then it is Super case-II transport, equal to 0.89, Case-II transport, between 0.45 and 0.89, Anomalous (nonFickian) diffusion or equal to 0.45, shows Fickian diffusion. All the data of dissolution studies was analyzed by using DD Solver [31, 36].

4. Results and Discussion

4.1. Sol–Gel Fraction. A decrease in gel fraction was observed while increasing the concentration of polymer (Table 1).

This reduction in gel fraction was observed because of the fact that when the concentration of the polymer increased, less cross linking took place that resulted in increase in un-reacted contents. Similar findings were reported in a study of Jalil et al. [30] where they synthesized the copolymer of sodium alginate and acrylic acid through free radical polymerization technique. They also reported the reduction in gel fraction with increase in concentration of polymer.

An increase in gel fraction was observed with increase in concentration of monomer or cross linking agent. This phenomenon was seen because of the fact that, an increase in proportion of monomer or cross linking agent resulted into more entanglement of polymer and monomer that led to higher degree of cross linking with less proportion of unreacted contents. These findings of our study also shown an agreement with a study performed by Sarfraz et al. [18] where they prepared hydrogel micro particles of β-cyclodextrin and methacrylic acid and reported an increase in gel fraction with increasing the proportion of monomer or cross linking agent.

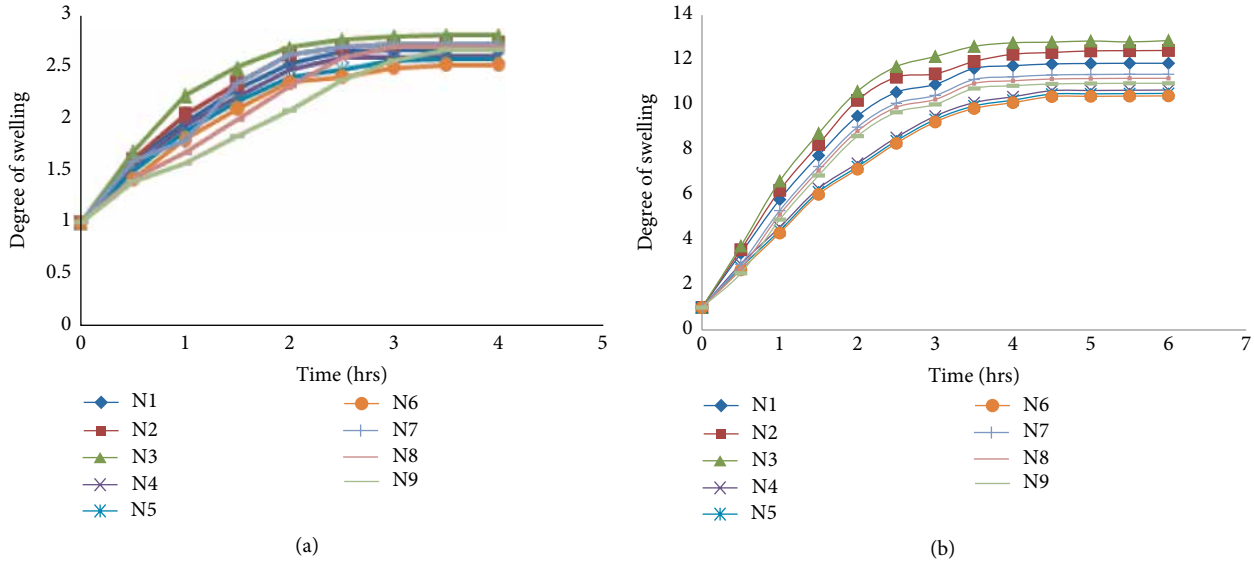

Figure 2: (a) Degree of swelling of formulation N1–N9 at pH 1.2. (b) Degree of swelling of formulation N1–N9 at pH 6.8.

Table 2: Entrapment efficiency and product yield of PEG-g-poly (MAA) nanogels.

Formulation	Entrapment efficiency (%)	Product yield (%)
N1	82.56 ± 0.24	90.00 ± 0.51
N2	82.87 ± 0.25	89.90 ± 0.27
N3	83.01 ± 0.23	92.00 ± 0.35
N4	84.89 ± 0.19	88.50 ± 0.42
N5	85.45 ± 0.18	87.10 ± 0.31
N6	88.40 ± 0.27	85.00 ± 0.32
N7	82.78 ± 0.21	87.10 ± 0.27
N8	81.98 ± 0.22	91.50 ± 0.21
N9	80.45 ± 0.27	87.70 ± 0.51

Average of three determinations, ±SD (standard deviation).

4.2. Swelling Behaviour. Prepared nanogels presented a pH dependent swelling behaviour as shown in Figures 2(a) and 2(b). At lower pH i.e. 1.2, formulation presented less swelling and appeared in condensed form. In acidic environment, due to high concentration of free hydrogen ions (H^+), carboxylic group of methacrylic acid (a weak acid) remain in unionized form as reported by Sarfraz et al. [18] and Elliot et al. [37]. Thus polymeric network remain in condensed form and less water is penetrated that lead to less swelling of nanogels.

At higher pH i.e. 6.8 a remarked increase in swelling was observed. This type of swelling behaviour was observed due to ionization of carboxylic group of methacrylic acid by releasing hydrogen ions (H^+) and thus attaining negative charge. Presence of successive negative charged groups resulted in activation of electrostatic repulsive forces that lead to the expansion of polymeric network and thus swelling of nanogels. Similar expansion of polymeric network was reported in a study performed by Tu et al. [38] due to ionization of the carboxylic group of the methacrylic acid at higher pH.

A decrease in swelling was observed when concentration of the monomer and cross linker was increased as shown in the case of formulations N4–N9. This decrease in swelling was seen because of the increase in cross linking density of formulations that resulted into decrease in water absorption capacity of nanogels and ultimately less swelling. A similar reduction in swelling with increasing the concentration of monomer was reported in studies performed by Rashid et al. [39] and Huang et al. [40]. Mahmood et al. [17] and Li and Mooney [41] also prepared methacrylic acid based hydrogel where with increase in concentration of monomer a decrease in swelling of hydrogel was observed.

4.3. Entrapment Efficiency and Product Yield. For the determination of efficiency of the prepared nanogels carrier systems, entrapment efficiency is considered as an important parameter. Results for entrapment efficiency of all prepared nanogels formulation is presented in Table 2 that ranges from 80.45% to 88.40%.

Results for product yield of all prepared nanogels were in the ranges of 85–92%. These results were in acceptable limit that depicted the good efficiency of process used for the synthesis of these formulations. These findings were in agreement with studies performed by Sarfraz et al. [25] and Mahmood et al. [31] where they prepared the β-cyclodextrin based hydrogel microparticulate system grafted with methacrylic acid and reported the good process efficiency as product yield was observed in the range of 85–93%.

4.4. Flow Properties. For formulations that are in powder form or particulate systems, determination of rheological parameters is very important in product development process. Materials with poor flow properties are not good candidates for use in solid dosage form thus may lead to improper mixing and loading of drugs as reported by Sarfraz et al. [18]. All the results for rheological parameters were found within pharmacopeial limits (Table 3). As the values of angle of repose ranged from 24.30θ to 28.9θ, (below 30) thus presented the good flow properties by all the prepared formulations. Similar results were reported in studies performed by Sarfraz et al. [25], Hafeezullah et al. [34], Singh and Sameer [42], and Minhas et al. [43].

Table 3: Results of micromeritics properties of formulations N1–N9.

Code	Bulk density (g/mL)	Tapped density (g/mL)	Angle of repose (θ)	Hausner's ratio	Carr's index (%)
N1	0.721	0.861	27.9	1.194	16.26
N2	0.642	0.743	26.5	1.157	13.59
N3	0.515	0.629	28.9	1.221	18.12
N4	0.701	0.831	26.8	1.186	15.64
N5	0.763	0.889	27.8	1.165	14.17
N6	0.804	0.963	26.4	1.198	16.51
N7	0.716	0.851	27.6	1.188	15.86
N8	0.749	0.872	28.1	1.164	14.10
N9	0.779	0.902	26.9	1.158	13.64

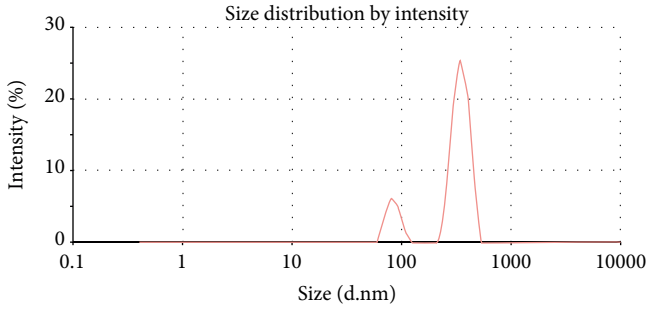

Figure 3: Average particles size of nanogels.

4.5. Particle Size Analysis. As depicted by peak size and peak area, particle size range for nanogels particulate system was 100–400 nm with maximum percentage at 300 nm (Figure 3). These results confirmed size of the prepared formulations in nano range as previously reported by Hamidi et al. [44] and Van Thienen et al. [45].

4.6. Zeta Potential. Zeta potential of prepared nanogels particulate system of formulation was neutral that demonstrate the stability of nanogels thus can be dispersed easily in aqueous media (Figure 4(a)). Results of this study also showed an agreement with a study performed by Tummala et al. [46] where they also reported the presence of net neutral charge on microparticulate system resulted into improvement in stability of the formulation.

When zeta potential of prepared formulations was studied at pH 6.8 (intestinal environment) it presented an increase in the value of zeta potential (Figure 4(b)). This increase in value of zeta potential is the indication of ionization of neutral surface of nanogels as previously reported by Cruz et al. [47] Presence of charges on the surface leads to electrostatic repulsion among similar charges and ultimately results into expansion of condensed structure.

4.7. FTIR Spectroscopic Analysis. Results for FTIR spectra is presented in Figures 5(a)–5(e). FTIR spectra of PEG-6000 presented the characteristic peaks at 1109 and 2870 cm^{-1} that was related to stretching of the ether group (C-O-C) and the alkyl group (R-CH_2) respectively. Absorption for hydroxyl group (OH) was indicated in the region of 3200–3300 cm^{-1} as reported previously by Mansur et al. [48]. FTIR spectra of MAA presented the characteristic peaks at 1708, 1635, and 2970 cm^{-1} that are corresponding to stretching of the carboxylic group (–C=O), double bond (C=C), and methyl group (–C–H) respectively. FTIR spectra of MBA presented the characteristic peaks at 1627 cm^{-1}, 1537 cm^{-1}, and 3228 that are related to stretching of the carbonyl group (C=O), amine group (NH), and methylene group (C=C–H) respectively.

FTIR spectra of grafted copolymeric nanogels of PEG-6000 (PEG-g-poly (MAA) presented the different absorption pattern as compared to individual ingredients. Disappearance of the absorption peak in region of 3200–3300 cm^{-1} and addition of new absorption peak in region of 1720–1730 cm^{-1} was observed that was corresponding to the involvement of the hydroxyl groups (OH) of PEG in the grafting process and addition of the carbonyl group (C=O) from monomer, MAA respectively. Results of this study also supported by findings of the study performed by Sarfraz et al. [25] where they prepared the β-CD-g-poly (MAA) hydrogels and confirmed the grafting process of copolymeric network system through disappearance of the characteristic peaks of the functional groups involved in the cross linking process.

FTIR spectra of naproxen sodium presented the absorption peaks at 1033 cm^{-1}, 1571 cm^{-1}, and 1670 cm^{-1} that were corresponding to the ether group (–OR), aromatic benzene ring, and carbonyl group (C=O) respectively. FTIR spectra of drug loaded formulations were also recorded and compare with spectra of the pure drug. This comparative analysis indicated that the drug (Naproxen) is in intact form as major peaks were in their original position i.e. 1033 cm^{-1} and 1571 cm^{-1} as in pure drug and the drug is physically entrapped in nanogels particulate systems as previously reported by Minhas et al. [43].

4.8. Thermal Analysis. Results for thermal analysis are presented in Figures 6(a) and 6(b). TGA curve of PEG presented an initial weight loss at 200°C that was because of the loss of moisture that presented a gradual mass loss and at 352°C only 12% mass of PEG was left. Similarly TGA curve of MBA showed the gradual mass loss at 187.64°C, 226.51°C, and 344.52°C. When degradation pathway of PEG-g-poly (MAA) nanogels (N3) was studied it showed the more thermal stability as compared to individual ingredients and even at higher temperature i.e. 401°C only 64% loss of mass occurred.

This improved thermal stability of prepared nanogels formulation also confirmed the grafting and development of copolymeric network systems that ultimately provided the targeted release of drug. Finding of TGA analysis also shown an agreement with the study performed by Mahmood et al. [17] and Chen et al. [49] where they confirmed the formation of the complex by improved thermal stability of chitosan based hydrogel.

A clear difference was observed in DSC thermogram of individual ingredients and nanogels formulations Figure 6(b). In DSC thermogram of PEG and MBA a specific pattern of endothermic peaks at 280°C and 212°C was observed that is followed by exothermic peaks at 358°C and 362°C respectively that indicating the loss of moisture content followed by thermal

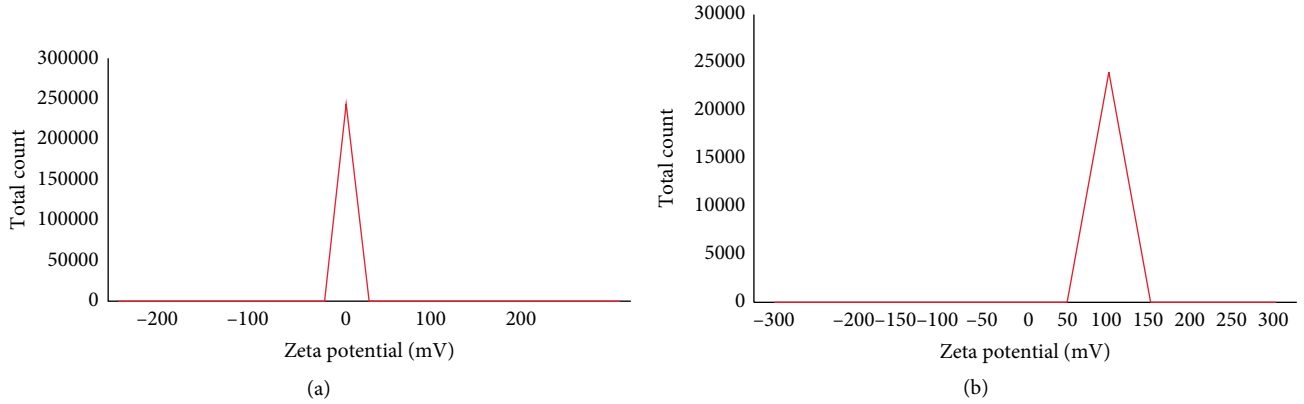

Figure 4: (a) Zeta potential measurement of nanogels in distilled water. (b) Zeta potential measurement of nanogels at pH 6.8.

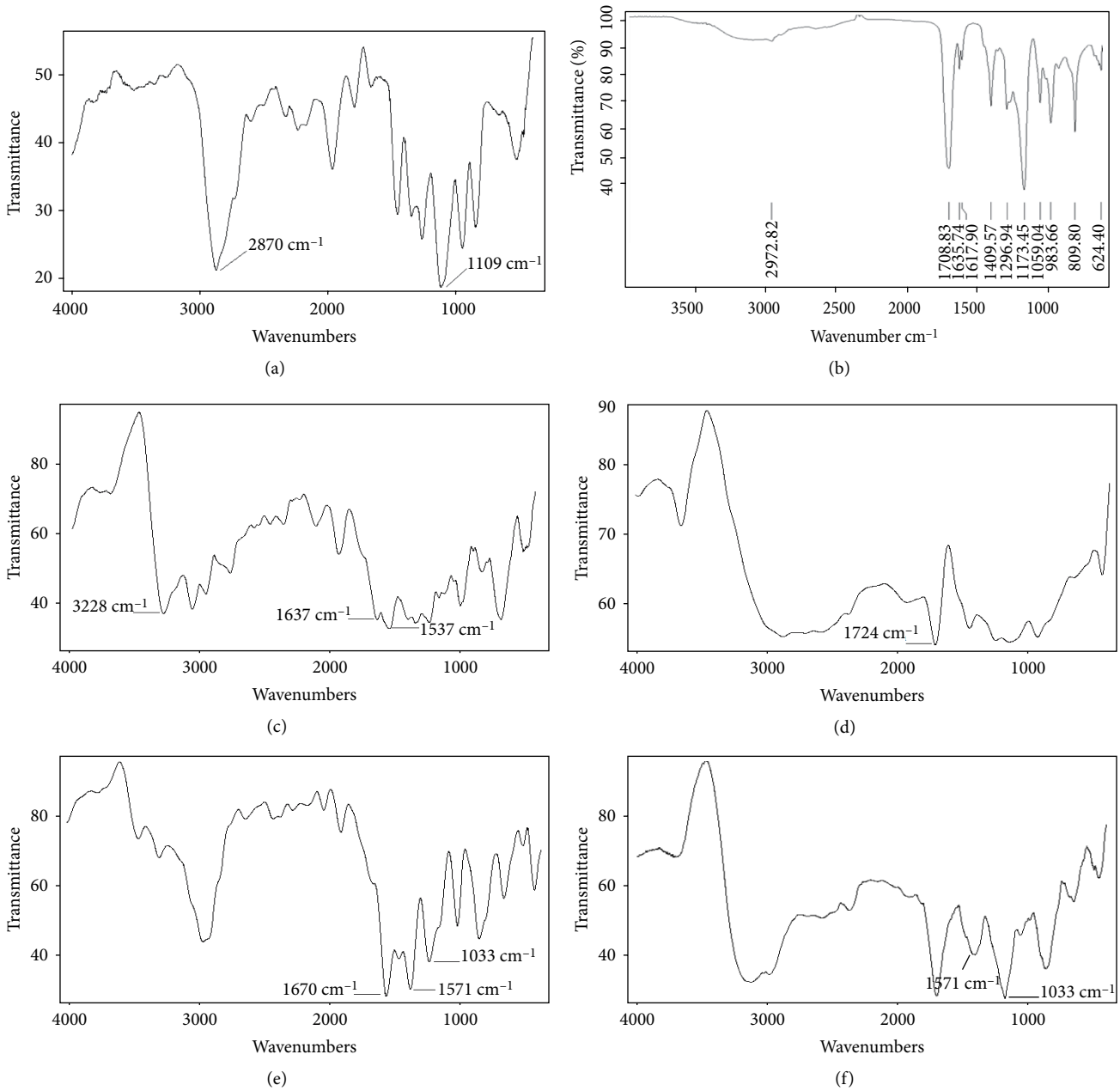

Figure 5: (a) FTIR spectra of PEG. (b) FTIR spectra of methacrylic acid. (c) FTIR spectra of MBA. (d) FTIR spectra of PEG-p (MAA). (e) FTIR spectra of naproxen sodium. (f) FTIR spectra of drug loaded nanogels.

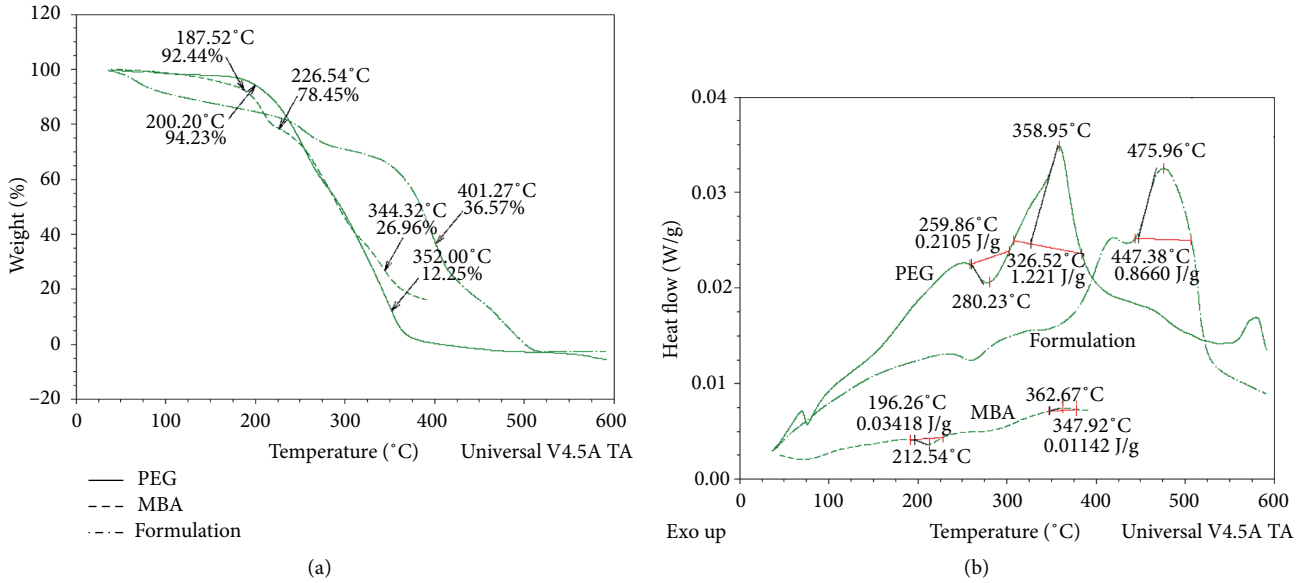

FIGURE 6: (a) TGA thermogram of PEG-6000, MBA, and PEG-g-poly (MAA) nanogels. (b) DSC thermogram of PEG-6000, MAA, and PEG-g-poly (MAA).

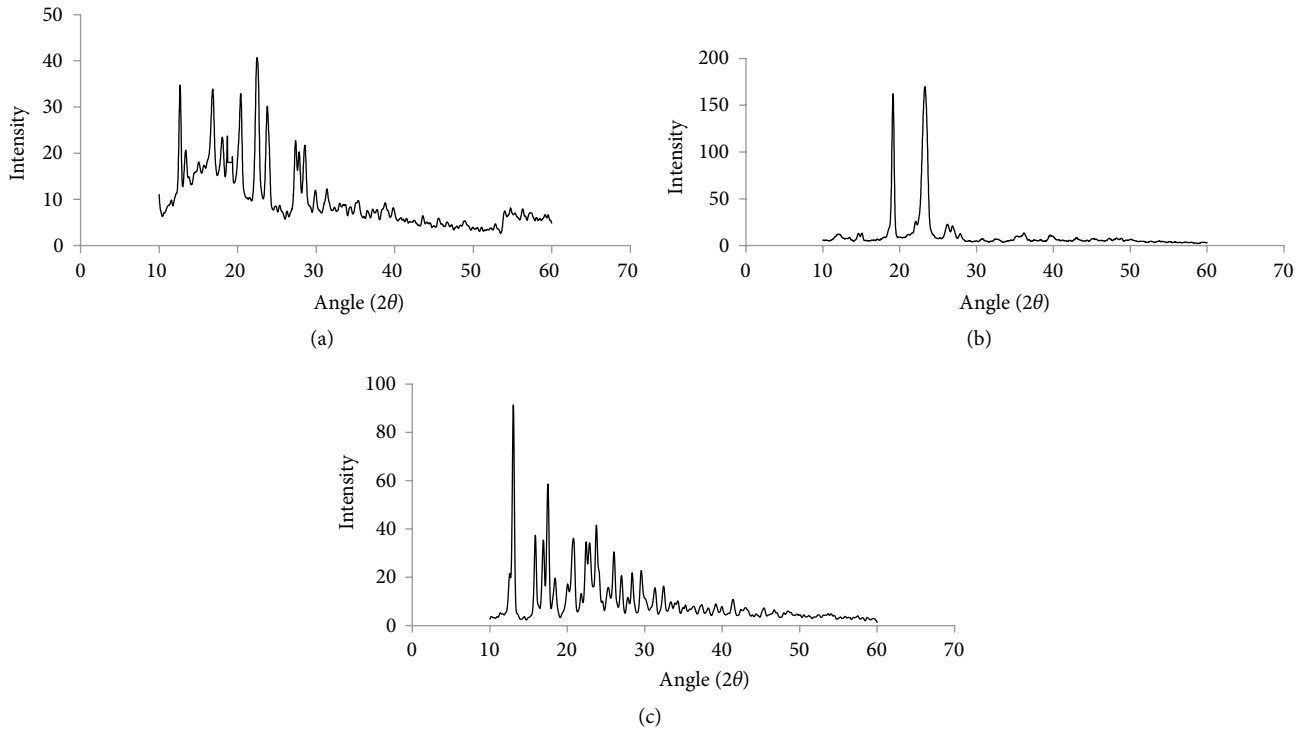

FIGURE 7: (a) XRD pattern of drug loaded PEG-g-poly (MAA) nanogels. (b) XRD pattern of PEG-6000. (c) XRD pattern of naproxen sodium.

degradation. While in DSC thermogram of nanogels formulations, endothermic peaks were present at 400°C followed by exothermic peaks at 475°C. This shifting of peaks toward higher temperature also confirmed the grafting and development of rigid copolymeric network systems. Similar result was reported in studies performed by Anwar et al. [50] where they prepared the alginate-PVA polymeric network systems and confirmed the grafting by indicating the shifting of exothermic peaks towards higher temperature. In another study performed by Jayaramudu et al. [51] improvement in thermal stability of PEG-6000 was reported when complexed with silver.

Thermal analysis of prepared formulation presented a better thermal stability as compared to individual ingredients that proposed a condensed structure for prepared nanogels. Such a condensed structure of prepared nanogels provided a better tool for targeted delivery of loaded drug.

Table 4: Models of *in-vitro* drug release kinetics of PEG-g-poly (MAA) nanogels formulations with varying concentration of polymer, PEG.

Model	Parameters	N1		N2		N3	
		pH 1.2	pH 6.8	pH 1.2	pH 6.8	pH 1.2	pH 6.8
Zero order	K_o	4.262	35.134	4.407	36.090	4.547	36.242
	R^2	0.6392	0.8944	0.5577	0.8602	0.4472	0.8848
First order	K_1	0.045	0.699	0.047	0.755	0.049	0.744
	R^2	0.6745	0.9714	0.5985	0.9705	0.4943	0.9606
Higuchi	K_H	6.473	52.002	6.724	53.646	6.975	53.691
	R^2	0.9707	0.9370	0.9526	0.9381	0.9195	0.9353
Korsmeyer Peppas	K_{Kp}	7.019	46.224	7.523	49.275	8.087	48.119
	R^2	0.9891	0.9598	0.9910	0.9510	0.9927	0.9551
	n	0.380	0.667	0.333	0.621	0.278	0.656

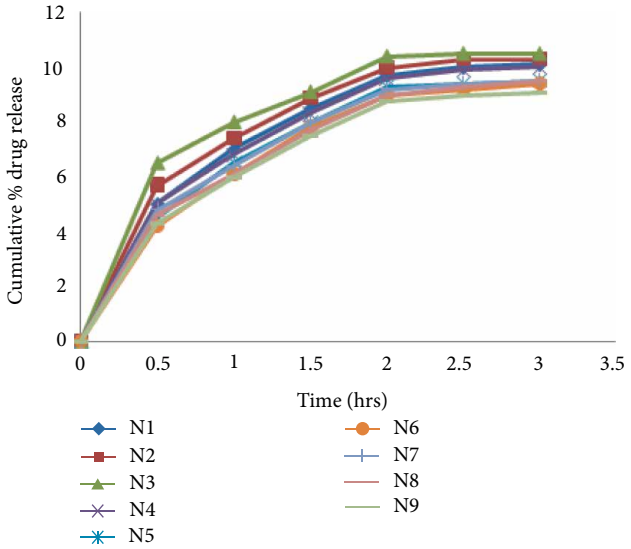

Figure 8: Cumulative percentage drug release from formulation (N1–N9) at pH 1.2.

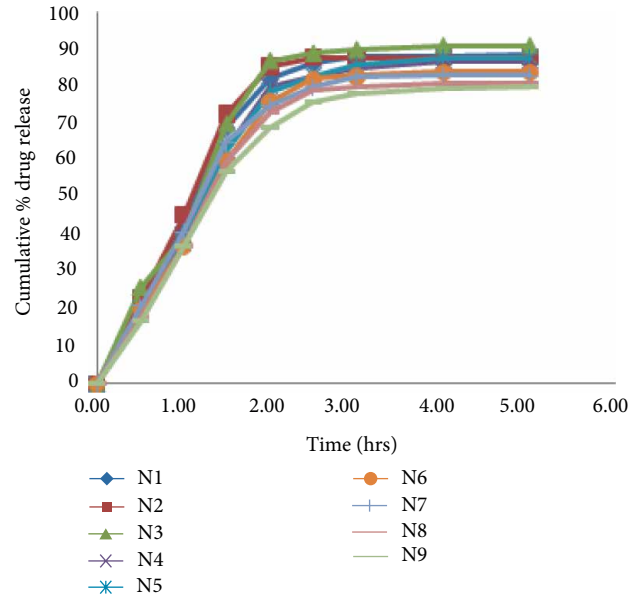

Figure 9: Cumulative percentage drug release from formulation (N1–N9) at pH 6.8.

4.9. Powder X-Rays Diffraction Studies. The diffractograms of pure drug presented the sharp peak at $2\theta = 13.04°$ and 17.5° while PEG-6000 at $2\theta = 19.1°$ that indicated the crystalline nature of these ingredients (Figures 7(a)–7(c)). There was no sharp peak in diffractograms of the nanogels copolymeric network that predicted the amorphous nature of these copolymeric network systems. Conversion of crystalline structure of polymers into amorphous form also confirmed the development of the grafted copolymeric networks. Similarly no sharp peaks were observed in diffraction patterns of the drug loaded nanogels that indicated the conversion of crystalline nature of naproxen sodium to amorphous nature. Conversion of crystalline nature of naproxen sodium into amorphous nature is also effective in the reduction of damaging effects of the drug to gastric mucosa as reported by Bodmeier and Chen [12].

4.10. In-Vitro Drug Release. A pH depended pattern of drug release was observed from prepared formulation as presented in Figures 8 and 9. Nanogels presented the drug release in the range of 8.2–10.5% at pH 1.2, while at higher pH i.e. 6.8, drug release is much high that is ranging from 80% to 91%. Maximum drug release was presented by formulation PM3 that was 91%. Such pH dependant release from these formulations was observed due to pH dependant swelling of these formulations. As at acidic pH, nanogels remain in collapse condition thus small amount of encapsulated drug was released but at pH 6.8, (intestinal pH) swelling of nanogels occurred that lead to higher release of drug. Such type of pH dependant pattern of drug release of this copolymeric network system made it a suitable candidate for gastro protective delivery of naproxen sodium as less drug was release in stomach pH and maximum drug was released at intestinal pH. Similar drug release was reported in studies performed by Peppas et al. [22] where they reported the gastro-protective delivery of insulin by using PMAA-g-EG nanogels carrier system. In another study performed by Sarfraz et al. [18], similar pH dependant release of rosuvastatin calcium was reported from β-cyclodextrin based hydrogel polymeric network system grafted with methacrylic acid.

Table 5: Models of *in-vitro* drug release kinetics of PEG-g-poly (MAA) nanogels formulations with varying concentration of MAA.

Model	Parameters	N4		N5		N6	
		pH 1.2	pH 6.8	pH 1.2	pH 6.8	pH 1.2	pH 6.8
Zero order	K_o	4.207	33.714	4.015	33.648	3.916	32.659
	R^2	0.6483	0.9085	0.6619	0.9220	0.7094	0.9237
First order	K_1	0.045	0.640	0.043	0.631	0.041	0.598
	R^2	0.6826	0.9736	0.6941	0.9693	0.7381	0.9756
Higuchi	K_H	6.386	49.800	6.090	49.572	5.922	48.145
	R^2	0.9731	0.9351	0.9711	0.9285	0.9792	0.9349
Korsmeyer Peppas	K_{Kp}	6.907	43.554	6.526	42.418	6.213	41.418
	R^2	0.9901	0.9634	0.9840	0.9648	0.9851	0.9691
	n	0.384	0.690	0.398	0.720	0.430	0.713

Table 6: Models of *in-vitro* drug release kinetics of PEG-g-poly (MAA) nanogels formulations with varying concentration of MBA.

Model	Parameters	N7		N8		N9	
		pH 1.2	pH 6.8	pH 1.2	pH 6.8	pH 1.2	pH 6.8
Zero order	K_o	4.009	32.813	3.943	31.626	3.815	30.462
	R^2	0.6420	0.8898	0.6917	0.9162	0.6872	0.9252
First order	K_1	0.042	0.619	0.042	0.567	0.040	0.529
	R^2	0.6749	0.9839	0.7214	0.9783	0.7163	0.9850
Higuchi	K_H	6.088	48.658	5.969	46.659	5.777	44.922
	R^2	0.9703	0.9486	0.9809	0.9335	0.9773	0.9393
Korsmeyer Peppas	K_{Kp}	6.595	43.932	6.341	40.401	6.134	38.761
	R^2	0.9881	0.9665	0.9905	0.9654	0.9867	0.9726
	n	0.382	0.646	0.411	0.704	0.412	0.708

Table 7: Comparison between swelling of all formulation at pH 1.2 and pH 6.8.

Code	Varying pH	Mean ± SEM	p-value	Sig. difference
N1	Degree of swelling at pH 1.2	2.36069 ± 0.15	0.0012	Yes
	Degree of swelling at pH 6.8	8.5308 ± 0.93		
N2	Degree of swelling at pH 1.2	2.41985 ± 0.15	0.0034	Yes
	Degree of swelling at pH 6.8	8.9151 ± 0.95		
N3	Degree of swelling at pH 1.2	2.50485 ± 0.15	0.0031	Yes
	Degree of swelling at pH 6.8	9.3701 ± 0. 93		
N4	Degree of swelling at pH 1.2	2.3103 ± 0. 15	0.0015	Yes
	Degree of swelling at pH 6.8	9.8958 ± 0.834		
N5	Degree of swelling at pH 1.2	2.2695 ± 0. 15	0.0012	Yes
	Degree of swelling at pH 6.8	10.389 ± 0. 93		
N6	Degree of swelling at pH 1.2	2.2109 ± 0. 15	0.0011	Yes
	Degree of swelling at pH 6.8	10.856 ± 0.829		
N7	Degree of swelling at pH 1.2	2.3993 ± 0. 15	0.0013	Yes
	Degree of swelling at pH 6.8	8.0408 ± 0. 96		
N8	Degree of swelling at pH 1.2	2.3023 ± 0. 15	0.0012	Yes
	Degree of swelling at pH 6.8	7.8608 ± 0. 94		
N9	Degree of swelling at pH 1.2	2.2230 ± 0. 15	0.0011	Yes
	Degree of swelling at pH 6.8	7.6408 ± 0.857		

4.11. Release Kinetics. Results for *in-vitro* drug release kinetics are presented in Tables 4–6. When dissolution data was evaluated with Higuchi model, results of drug release found the best fit model to regression line with values of R^2 more close to one. On the basis of these observations it was concluded that the best fit model for the mechanism of drug release from nanogels carrier systems was Higuchi model as value of R^2 was found more close to one at both pH values.

Table 8: Comparison between drug release of all formulation at pH 1.2 and pH 6.8.

Code	Varying pH	Mean ± SEM	p-value	Sig. difference
N1	Drug release at pH 1.2	6.7 ± 1.5	0.001	Yes
	Drug release at pH 6.8	62 ± 11		
N2	Drug release at pH 1.2	7.05 ± 1.6	0.001	Yes
	Drug release at pH 6.8	64.3 ± 11		
N3	Drug release at pH 1.2	7.42 ± 1.6	0.001	Yes
	Drug release at pH 6.8	64.9 ± 11		
N4	Drug release at pH 1.2	7.09 ± 1.4	0.001	Yes
	Drug release at pH 6.8	51.5 ± 9.2		
N5	Drug release at pH 1.2	6.74 ± 1.3	0.001	Yes
	Drug release at pH 6.8	51.1 ± 9.4		
N6	Drug release at pH 1.2	6.53 ± 1.3	0.001	Yes
	Drug release at pH 6.8	49.5 ± 8.9		
N7	Drug release at pH 1.2	6.76 ± 1.3	0.001	Yes
	Drug release at pH 6.8	50.6 ± 8.8		
N8	Drug release at pH 1.2	6.6 ± 1.3	0.001	Yes
	Drug release at pH 6.8	48.3 ± 8.7		
N9	Drug release at pH 1.2	6.39 ± 1.3	0.001	Yes
	Drug release at pH 6.8	46.5 ± 8.4		

On the basis of values of "n" it was concluded that all formulation follow anomalous i.e. dual mode of drug release (non-Fickian diffusion) as values of "n" lying between 0.45 and 0.89 for all formulations.

4.12. Statistical Analysis of Swelling Behaviour and Drug Release. Swelling data and drug release data was also analysed statistically by using Minitab software and results are presented in Tables 7 and 8.

From statistical analysis it was concluded that a significance difference in drug release was observed for all formulation at different pH values. These results also justified that prepared formulations are pH sensitive in nature.

5. Conclusion

In the current study copolymeric nanogels carrier systems were formulated for gastro-protective delivery of naproxen sodium. Polyethylene glycol was grafted with varying concentration of a monomer, methacrylic acid respectively through free radical polymerization technique. Nanogels carrier systems presented the pH dependent swelling behaviour with maximum swelling index at higher pH i.e. 6.8. PXRD studies of drug loaded formulation indicated the amorphous nature of carrier systems and loaded drug irrespective to the crystalline nature of individual ingredients that is effective in the improvement in the bioavailability as well as reduced irritant effect of the drug to the mucosal membrane of GIT. Nanogels carrier systems also presented the pH dependent drug release with maximum release at a higher pH i.e. 6.8 and less release at a lower pH i.e. 1.2 thus by-passed the acidic environment for drug release. On the basis of these investigation, it was concluded that these nanogels carrier systems proved to be an effective tool for the gastro-protective delivery of drug molecules that are gastric irritant like naproxen sodium. Further studies are required for the evaluation of *in-vivo* safety and efficacy of prepared nanogels carrier system in order to establish a safe, effective, and economic gastro-protective oral drug delivery system for gastric irritant drugs.

Data Availability

Data should be available openly.

Conflicts of Interest

The authors declare that they have no conflicts of interest.

References

[1] C. S. Sean and B. Paul, Ed., *Martindale, The Complete Drug Reference*, pp. 1693–1699, Pharmaceutical Press, London, 36th edition, 2009.

[2] B. K. Alldredge, R. L. Corelli, M. E. Ernst et al., *Koda-kimble and Young's Applied Therapeutics: The Clinical Use of Drugs*, pp. 661–667, Wolters Kluwer Health Adis (ESP), Alphen aan den Rijn, Netherlands, 10th edition, 2013.

[3] A. H. Soll, K. John, and J. E. McGuigan, "Ulcers, nonsteroidal antiinflammatory drugs, and related matters," *Gastroenterology*, vol. 96, no. 2, pp. 561–568, 1989.

[4] D. L. Earnest, "NSAID-induced gastric injury: its pathogenesis and management," *Seminars in Arthritis and Rheumatism*, vol. 19, no. 4 Suppl 2, pp. 6–10, 1990.

[5] G. G. Liversidge and P. Conzentino, "Drug particle size reduction for decreasing gastric irritancy and enhancing absorption of naproxen in rats," *International Journal of Pharmaceutics*, vol. 125, no. 2, pp. 309–313, 1995.

[6] A. Lanas and F. Sopeña, "Nonsteroidal anti-inflammatory drugs and lower gastrointestinal complications," *Gastroen-*

terology Clinics of North America, vol. 38, no. 2, pp. 333–352, 2009.

[7] V. R. Shanbhag, A. M. Crider, R. Gokhale, A. Harpalani, and M. D. Ronald, "Ester and amide prodrugs of ibuprofen and naproxen: synthesis, anti-inflammatory activity, and gastrointestinal toxicity," *Journal of Pharmaceutical Sciences*, vol. 81, no. 2, pp. 149–154, 1992.

[8] P. C. Sharma, S. Yadav, R. Pahwa, D. Kaushik, and S. Jain, "Synthesis and evaluation of novel prodrugs of naproxen," *Medicinal Chemistry Research*, vol. 20, no. 5, pp. 648–655, 2011.

[9] J. Sharma, A. K. Singla, and S. Dhawan, "Zinc–naproxen complex: synthesis, physicochemical and biological evaluation," *International Journal of Pharmaceutics*, vol. 260, no. 2, pp. 217–227, 2003.

[10] R. C. Mundargi, S. A. Patil, P. V. Kulkarni, N. N. Mallikarjuna, and T. M. Aminabhavi, "Sequential interpenetrating polymer network hydrogel microspheres of poly (methacrylic acid) and poly (vinyl alcohol) for oral controlled drug delivery to intestine," *Journal of Microencapsulation*, vol. 25, no. 4, pp. 228–240, 2008.

[11] I. Khalid, M. Ahmad, M. Usman Minhas, K. Barkat, and M. Sohail, "Cross-linked sodium alginate-g-poly (acrylic acid) structure: a potential hydrogel network for controlled delivery of loxoprofen sodium," *Advances in Polymer Technology*, vol. 37, no. 4, pp. 985–995, 2018.

[12] R. Bodmeier and H. Chen, "Preparation and characterization of microspheres containing the anti-inflammatory agents, indomethacin, ibuprofen, and ketoprofen," *Journal of Controlled Release*, vol. 10, no. 2, pp. 167–175, 1989.

[13] N. H. Stacey and C. Winder, "Toxicity of organic solvents," *Occupational Toxicology*, pp. 364–389, CRC Press, Boca Raton, FL, USA, 2004.

[14] L. Liu, W. D. Yao, Y. F. Rao, X. Y. Lu, and J. Q. Gao, "pH-responsive carriers for oral drug delivery: challenges and opportunities of current platforms," *Drug Delivery*, vol. 24, no. 1, pp. 569–581, 2017.

[15] A. V. Kabanov and S. V. Vinogradov, "Nanogels as pharmaceutical carriers: finite networks of infinite capabilities," *Angewandte Chemie International Edition*, vol. 48, no. 30, pp. 5418–5429, 2009.

[16] H. Q. Wu and C. C. Wang, "Biodegradable smart nanogels: a new platform for targeting drug delivery and biomedical diagnostics," *Langmuir*, vol. 32, no. 25, pp. 6211–6225, 2016.

[17] A. Mahmood, M. Ahmad, R. M. Sarfraz, and M. U. Minhas, "Development of acyclovir loaded β-cyclodextrin-g-poly methacrylic acid hydrogel microparticles: an *in vitro* characterization," *Advances in Polymer Technology*, vol. 37, no. 3, pp. 697–705, 2018.

[18] R. M. Sarfraz, M. Ahmad, A. Mahmood, and H. Ijaz, "Development, *in vitro* and *in vivo* evaluation of pH responsive β-CD-comethacrylic acid-crosslinked polymeric microparticulate system for solubility enhancement of rosuvastatin calcium," *Polymer-Plastics Technology and Engineering*, vol. 57, no. 12, pp. 1175–1187, 2018.

[19] J. P. K. Tan, A. Q. F. Zeng, C. C. Chang, and K. C. Tam, "Release kinetics of procaine hydrochloride (PrHy) from pH-responsive nanogels: theory and experiments," *International Journal of Pharmaceutics*, vol. 357, no. 1-2, pp. 305–313, 2008.

[20] I. Neamtu, A. G. Rusu, A. Diaconu, L. E. Nita, and A. P. Chiriac, "Basic concepts and recent advances in nanogels as carriers for medical applications," *Drug Delivery*, vol. 24, no. 1, pp. 539–557, 2017.

[21] C. W. Park, H. M. Yang, H. J. Lee, and J. D. Kim, "Core–shell nanogel of PEG–poly (aspartic acid) and its pH-responsive release of rh-insulin," *Soft Matter*, vol. 9, no. 6, pp. 1781–1788, 2013.

[22] N. A. Peppas, B. K. Kelley, T. L. Madeline, and A. M. Lowman, "Poly (ethylene glycol)-containing hydrogels in drug delivery," *Journal of Controlled Release*, vol. 62, no. 1-2, pp. 81–87, 1999.

[23] N. A. Peppas, "Devices based on intelligent biopolymers for oral protein delivery," *International Journal of Pharmaceutics*, vol. 277, no. 1-2, pp. 11–17, 2004.

[24] F. Zaaeri, M. Khoobi, M. Rouini, and H. A. Javar, "pH-responsive polymer in a core–shell magnetic structure as an efficient carrier for delivery of doxorubicin to tumor cells," *International Journal of Polymeric Materials and Polymeric Biomaterials*, vol. 67, no. 16, pp. 967–977, 2018.

[25] R. M. Sarfraz, M. Ahmad, A. Mahmood, M. U. Minhas, and A. Yaqoob, "Development and evaluation of rosuvastatin calcium based microparticles for solubility enhancement: an *in vitro* study," *Advances in Polymer Technology*, vol. 36, no. 4, pp. 433–441, 2017.

[26] A. M. Lowman, M. Morishita, M. Kajita, T. Nagai, and N. A. Peppas, "Oral delivery of insulin using pH-responsive complexation gels," *Journal of Pharmaceutical Sciences*, vol. 88, no. 9, pp. 933–937, 1999.

[27] S. Sajeesh and C. P. Sharma, "Interpolymer complex microparticles based on polymethacrylic acid-chitosan for oral insulin delivery," *Journal of Applied Polymer Science*, vol. 99, no. 2, pp. 506–512, 2006.

[28] B. K. Deka and T. K. Maji, "Effect of coupling agent and nanoclay on properties of HDPE, LDPE, PP, PVC blend and Phargamites karka nanocomposite," *Composites Science and Technology*, vol. 70, no. 12, pp. 1755–1761, 2010.

[29] M. Sohail, M. Ahmad, M. U. Minhas, L. Ali, I. Khalid, and H. Rashid, "Controlled delivery of valsartan by cross-linked polymeric matrices: synthesis, *in vitro* and *in vivo* evaluation," *International Journal of Pharmaceutics*, vol. 487, no. 1-2, pp. 110–119, 2015.

[30] A. Jalil, S. Khan, F. Naeem et al., "The structural, morphological and thermal properties of grafted pH-sensitive interpenetrating highly porous polymeric composites of sodium alginate/acrylic acid copolymers for controlled delivery of diclofenac potassium," *Designed Monomers and Polymers*, vol. 20, no. 1, pp. 308–324, 2017.

[31] A. Mahmood, M. Ahmad, R. M. Sarfraz, and M. U. Minhas, "β-CD based hydrogel microparticulate system to improve the solubility of acyclovir: optimization through *in-vitro, in-vivo* and toxicological evaluation," *Journal of Drug Delivery Science and Technology*, vol. 36, pp. 75–88, 2016.

[32] N. T. T. Huyen, N. H. Nhung, L. Thanh, P. D. Khanh, T. D. Lam, and H. A. Son, "Preparation and characterization of zerovalent iron nanoparticles," *Vietnam Journal of Chemistry*, vol. 56, no. 2, pp. 226–230, 2018.

[33] T. Di Francesco and G. Borchard, "A robust and easily reproducible protocol for the determination of size and size distribution of iron sucrose using dynamic light scattering," *Journal of Pharmaceutical and Biomedical Analysis*, vol. 152, pp. 89–93, 2018.

[34] K. Hafeezullah, A. Mahmood, S. Maheen et al., "Formulation and *in vitro* evaluation of novel antidiabetic orodispersible tablets using kyron-T134 and crosscaramellose sodium as superdisintegrants," *Lattin Aerican Journal of Pharmacy*, vol. 33, no. 4, pp. 631–639, 2014.

[35] R. M. Sarfraz, H. U. Khan, A. Mahmood, M. Ahmad, S. Maheen, and M. Sher, "Formulation and evaluation of mouth disintegrating tablets of atenolol and atorvastatin," *Indian Journal of Pharmaceutical Sciences*, vol. 77, no. 1, p. 83, 2015.

[36] S. Khan, M. Ahmad, G. Murtaza et al., "Formulation of nimesulide floating microparticles using low-viscosity hydroxypropyl methylcellulose," *Tropical Journal of Pharmaceutical Research*, vol. 9, no. 3, 2010.

[37] J. E. Elliott, M. Macdonald, J. Nie, and C. N. Bowman, "Structure and swelling of poly (acrylic acid) hydrogels: effect of pH, ionic strength, and dilution on the crosslinked polymer structure," *Polymer*, vol. 45, no. 5, pp. 1503–1510, 2004.

[38] H. Tu, Y. Yu, J. Chen et al., "Highly cost-effective and high-strength hydrogels as dye adsorbents from natural polymers: chitosan and cellulose," *Polymer Chemistry*, vol. 8, no. 19, pp. 2913–2921, 2017.

[39] H. Rashid, M. Ahmad, M. U. Minhas, M. Sohail, and M. F. Aamir, "Synthesis and characterization of poly (hydroxyethyl methacrylate-co-methacrylic acid) cross linked polymeric network for the delivery of analgesic agent," *Journal of the Chemical Society of Pakistan*, vol. 37, no. 5, pp. 999–1007, 2015.

[40] S. Huang, J. Wang, and Q. Shang, "Development and evaluation of a novel polymeric hydrogel of sucrose acrylate-co-polymethylacrylic acid for oral curcumin delivery," *Journal of Biomaterials Science, Polymer Edition*, vol. 28, no. 2, pp. 194–206, 2017.

[41] J. Li and D. J. Mooney, "Designing hydrogels for controlled drug delivery," *Nature Reviews Materials*, vol. 1, no. 12, p. 16071, 2016.

[42] S. K. Singh and A. A. Sameer, "Development and characterization of sublingual tablet of Lisinopril," *Asian Pacific Journal of Tropical Biomedicine*, vol. 2, no. 3, pp. S1711–S1719, 2012.

[43] M. U. Minhas, M. Ahmad, L. Ali, and M. Sohail, "Synthesis of chemically cross-linked polyvinyl alcohol-co-poly (methacrylic acid) hydrogels by copolymerization; a potential graft-polymeric carrier for oral delivery of 5-fluorouracil," *DARU Journal of Pharmaceutical Sciences*, vol. 21, no. 1, p. 44, 2013.

[44] M. Hamidi, A. Azadi, and P. Rafiei, "Hydrogel nanoparticles in drug delivery," *Advanced Drug Delivery Reviews*, vol. 60, no. 15, pp. 1638–1649, 2008.

[45] T. G. Van Thienen, J. Demeester, and S. C. De Smedt, "Screening poly (ethyleneglycol) micro-and nanogels for drug delivery purposes," *International Journal of Pharmaceutics*, vol. 351, no. 1-2, pp. 174–185, 2008.

[46] S. Tummala, M. N. S. Kumar, and A. Prakash, "Formulation and characterization of 5-Fluorouracil enteric coated nanoparticles for sustained and localized release in treating colorectal cancer," *Saudi Pharmaceutical Journal*, vol. 23, no. 3, pp. 308–314, 2015.

[47] D. L. Cruz, E. Francisco, Y. Zheng et al., "Zeta potential of modified multi-walled carbon nanotubes in presence of poly (vinyl alcohol) hydrogel," *International Journal of Electrochemical Sciences*, vol. 7, pp. 3577–3590, 2012.

[48] H. S. Mansur, R. L. Oréfice, and A. A. P. Mansur, "Characterization of poly (vinyl alcohol)/poly (ethylene glycol) hydrogels and PVA-derived hybrids by small-angle X-ray scattering and FTIR spectroscopy," *Polymer*, vol. 45, no. 21, pp. 7193–7202, 2004.

[49] C. Chang, Z. C. Wang, C. Y. Quan et al., "Fabrication of a novel pH-sensitive glutaraldehyde cross-linked pectin nanogel for drug delivery," *Journal of Biomaterials Science, Polymer Edition*, vol. 18, no. 12, pp. 1591–1599, 2007.

[50] H. Anwar, M. Ahmad, M. U. Minhas, and S. Rehmani, "Alginate-polyvinyl alcohol based interpenetrating polymer network for prolonged drug therapy, optimization and *in-vitro* characterization," *Carbohydrate polymers*, vol. 166, pp. 183–194, 2017.

[51] T. Jayaramudu, G. M. Raghavendra, K. Varaprasad et al., "Preparation and characterization of poly(ethylene glycol) stabilized nano silver particles by a mechanochemical assisted ball mill process," *Journal of Applied Polymer Science*, vol. 133, no. 7, 2016.